

# OBSERVING THE BUILDING BLOCKS OF PLANETS

## IN PROTOPLANETARY DISKS

incl. L.B.F.M. Waters<sup>3,4</sup>, M. Hogerheijde<sup>2,5</sup>, R. van Boekel<sup>6</sup>, A. Matter<sup>7</sup>, B. Lopez<sup>7</sup>, K. Perraut<sup>8</sup>, C. Dominik<sup>5</sup>, L. Chen<sup>1</sup>, Á. Kóspál<sup>1,6</sup>, P. Ábrahám<sup>1</sup>, and the GRAVITY collaboration

<sup>1</sup> Konkoly Observatory, CSFK, Budapest, Hungary  
e-mail: varga.jozsef@csfk.org

<sup>2</sup> Leiden Observatory, Leiden University, The Netherlands

<sup>3</sup> Institute for Mathematics, Astrophysics and Particle Physics, Radboud University, Nijmegen, The Netherlands

<sup>4</sup> SRON Netherlands Institute for Space Research, Leiden, The Netherlands

<sup>5</sup> Anton Pannekoek Institute for Astronomy, University of Amsterdam, The Netherlands

<sup>6</sup> MPA, Heidelberg, Germany

<sup>7</sup> Laboratoire Lagrange, Université Côte d'Azur, OCA, CNRS, Nice, France

<sup>8</sup> Université Grenoble Alpes, CNRS, IPAG, France

Terrestrial planets which form in the inner few au region of protoplanetary disks, acquire most of their mass from solids, originally in the form of small  $\mu\text{m}$ -sized dust grains made of silicates, carbon, iron, etc. Cosmic silicate grains can be easily detected at mid-infrared wavelengths, by their characteristic spectral features (Fig. 2). Spectral analysis can uncover the mineral buildup of the dust, and thus we can estimate the composition of the planets forming from that material, and make comparisons with our Solar System.

### OBSERVATIONS

We present Very Large Telescope Interferometer (VLTI, Fig. 1) observations on the planet-forming disk around the young star HD 144432. VLTI instruments can detect and spatially resolve the warm and hot dust in the inner disk region ( $r \lesssim 10$  au) where terrestrial planets can form. We used data from the PIONIER (H-band), GRAVITY (K-band), and MATISSE (LMN-bands) instruments to model the disk of HD 144432. MATISSE is uniquely suited for constraining the composition and spatial distribution of silicates, because of its coverage of the N-band silicate spectral feature (Fig. 2).

### DISK MODEL

Our model is a flat-disk temperature gradient model divided into several radial zones, where each zone has its own surface density profile. Within our model, a spectral decomposition is applied to the MATISSE N-band data, in order to constrain the abundances of various silicate dust components.

### RESULTS

The best fit model image shows a three-ringed disk structure, with ring inner radii at  $0.2 \pm 0.03$  au,  $1.3 \pm 0.1$  au, and  $4.1 \pm 0.2$  au (Fig. 2). The bulk of the silicate emission originates in the second disk zone, between 1.3 and 4.1 au (Figs. 3, 4). The inner disk zone ( $< 1.3$  au) has much higher crystalline dust content, compared to the outer zones (Fig. 5). This suggests significant dust processing, probably due to thermal processes in the innermost disk zone. We found that the disk emission is optically thin in the inner two zones ( $< 4.1$  au) at thermal infrared wavelengths. Our results highlight the power of mid-infrared spectro-interferometry in constraining the composition and distribution of dust in disks, and show the most detailed view on the terrestrial planet forming region of a circumstellar disk obtained so far.

**Fig. 2.** Best-fit model image of the disk of HD 144432 at  $8.3 \mu\text{m}$  wavelength, showing three rings with inner radii at 0.2, 1.3, and 4.1 au. The central star is not shown. The disk is slightly inclined.

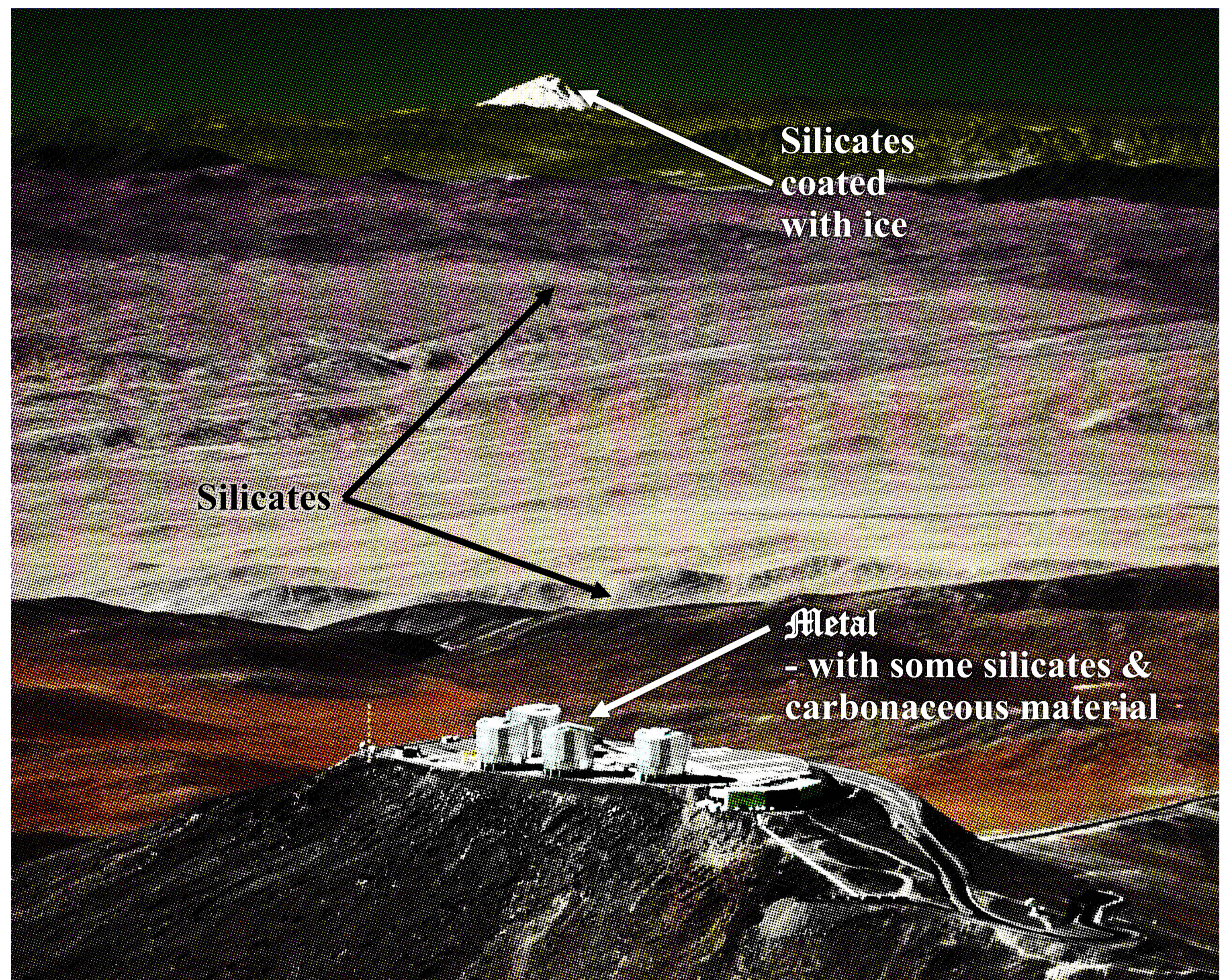
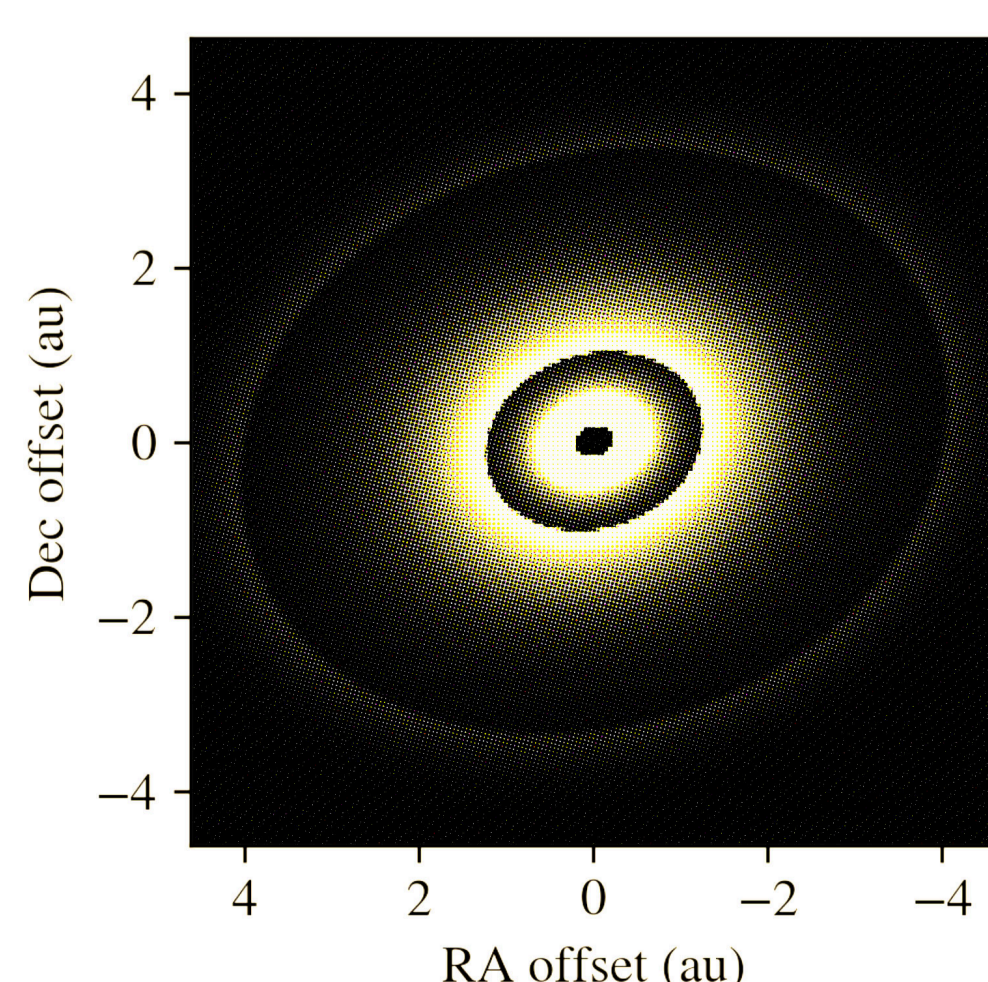


**Fig. 1.** Observations were taken with the Very Large Telescope Interferometer (VLTI) located at ESO's Paranal Observatory, Chile. VLTI instruments sample the Fourier-transform of an object's image on the sky (the so-called visibility function). Credit: ESO/G.Hüdepohl (atacamaphoto.com)

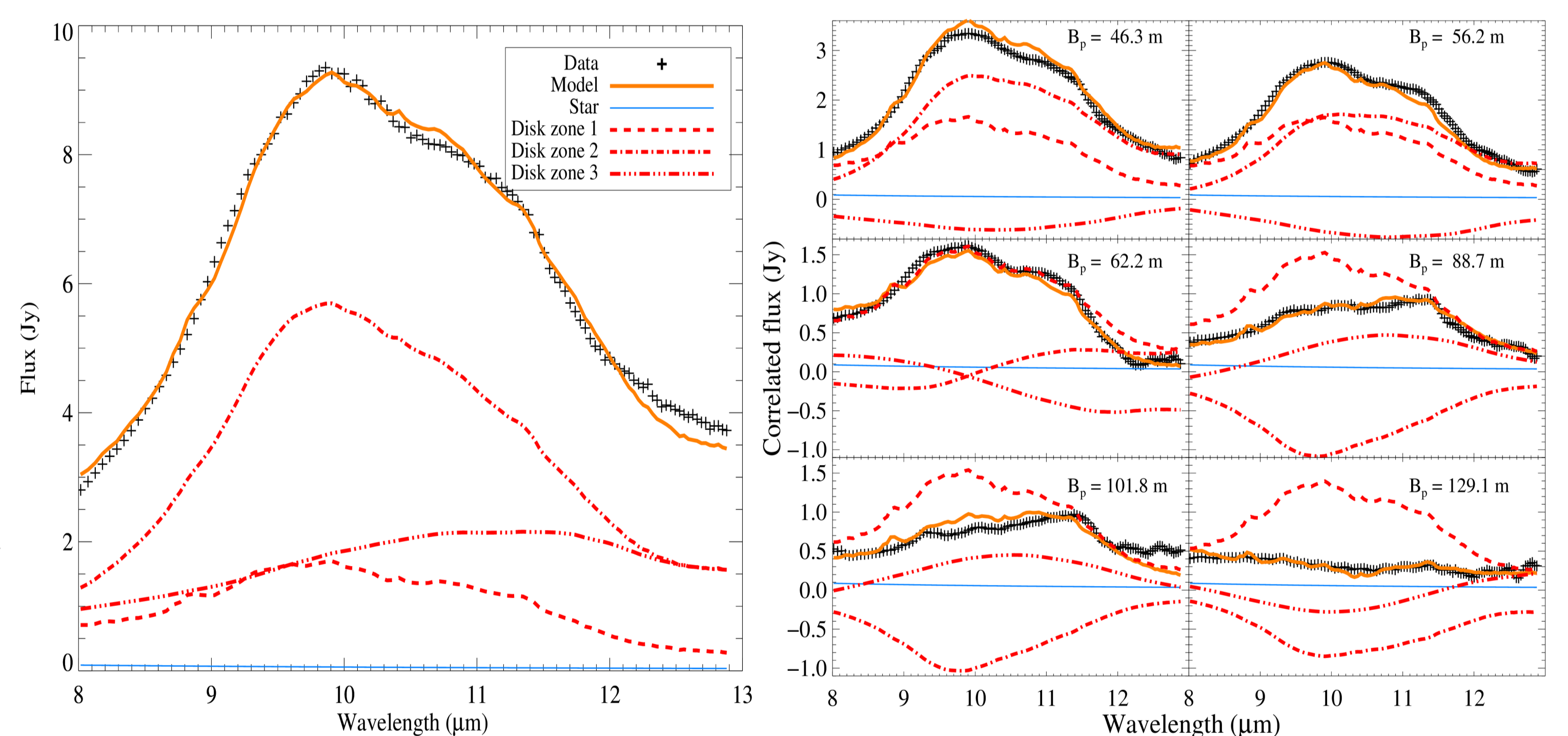


**Fig. 3.** VLTI/MATISSE data on HD 144432: N-band single-dish spectrum (left panel), and interferometric (correlated) spectra sampled at 6 baselines (right panel). The silicate spectral feature dominates the emission. The contributions of the three disk zones are the red lines, while the total fit to that data is shown in orange. The correlated spectra are not proper spectra, but they show the spatial signature of the object (visibility function in flux units), sampled at various baselines.

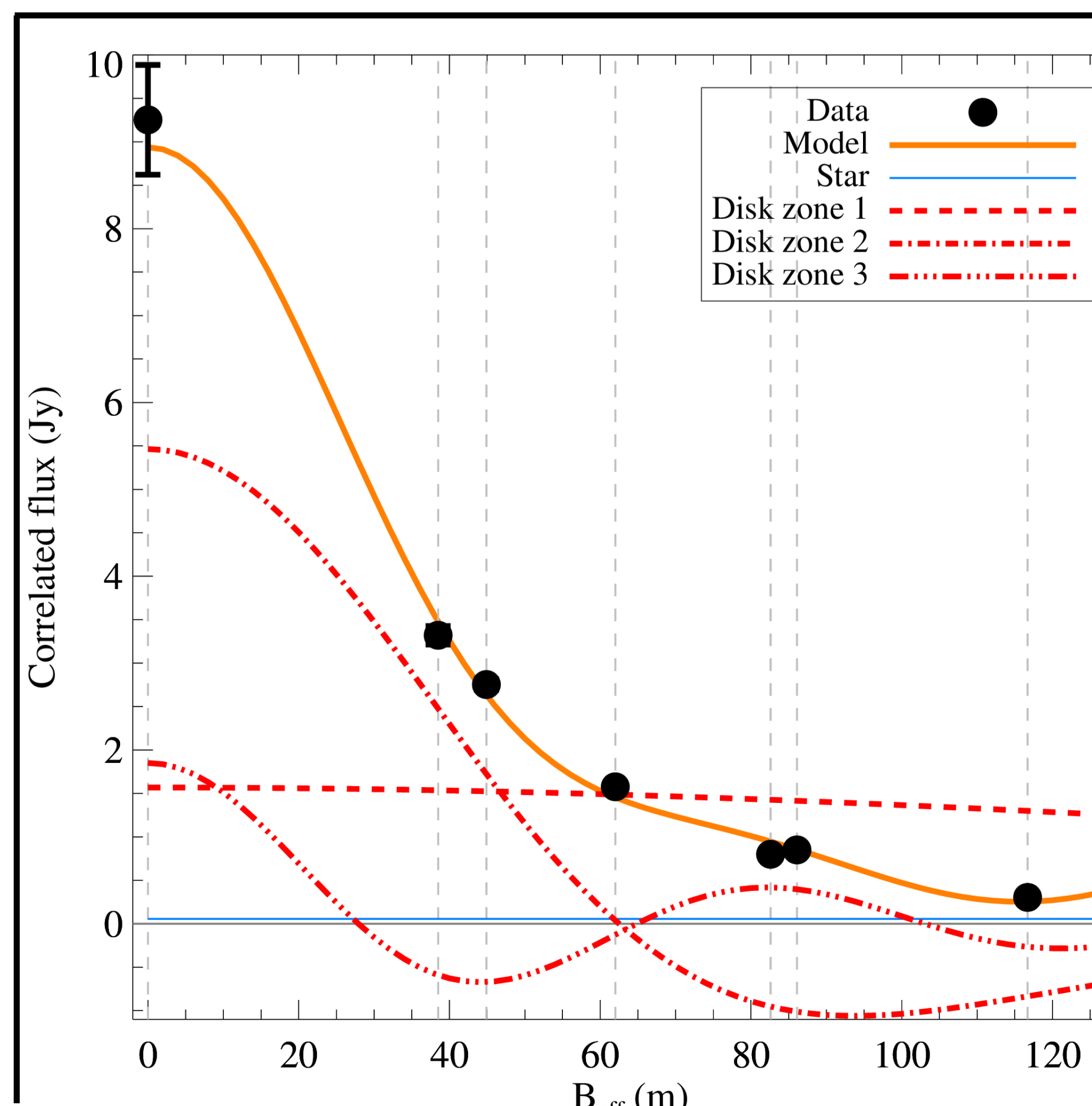
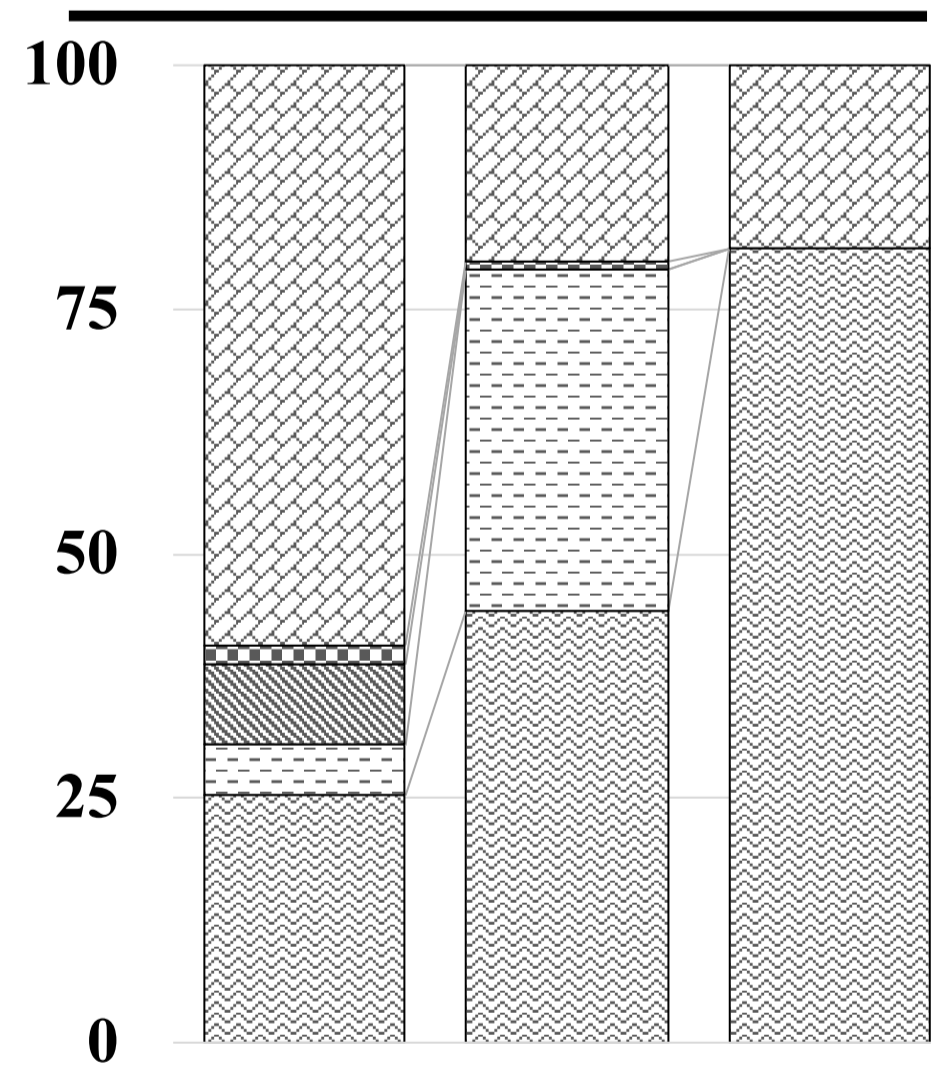


**Fig. 4.** Correlated flux density as function of the baseline length at a selected wavelength,  $10 \mu\text{m}$ . As the disk gets more resolved with increasing baseline length, the correlated flux decreases. The contributions of the various disk zones (red lines) show the effects of resolution: while the correlated flux of the inner zone barely decreases in the sampled baseline range, the other two zones show a sharper decrease, and a wavy pattern. The frequency of this pattern is related to the location of the zones: the further out a ring is located, the higher is the frequency. The contributions of the disk zones are added up to obtain the correlated flux of the full disk (orange line). The zero-baseline correlated flux is just the single-dish flux. Note that the correlated flux (= real value of the complex visibility) may have negative values.



0.2-1.3 au    1.3-4.1 au    > 4.1 au

- Enstatite 5.0  $\mu\text{m}$
- Forsterite 0.1  $\mu\text{m}$
- Pyroxene 2.0  $\mu\text{m}$
- Pyroxene 0.1  $\mu\text{m}$
- Olivine 2.0  $\mu\text{m}$

**Fig. 5.** Mass fractions of the silicate dust components, constrained by our model. The most abundant species are amorphous olivine ( $2 \mu\text{m}$ ), crystalline enstatite ( $5 \mu\text{m}$ ), and amorphous pyroxene ( $0.1 \mu\text{m}$ ). The fractions in the third disk zone are not well constrained.

